An investigation of the stepped thermography technique for defects evaluation in GFRP materials

NDT& E International post-print

DOI: https://doi.org/10.1016/j.ndteint.2018.12.011

An investigation of the stepped thermography technique for defects evaluation in GFRP materials

Davide Palumbo*, Pasquale Cavallo, Umberto Galietti

Department of Mechanics, Mathematics and Management (DMMM), Politecnico di Bari, Viale Japigia 182, 70126, Bari (Italy)

Corresponding author: *Davide Palumbo. Email: davide.palumbo@poliba.it

Abstract

The ability of thermography to detect defects in composite materials has been demonstrated and showed in various works and in many applications. In this regard, various NDT techniques are currently used for defect detection in composites such as Lock-in Thermography (LT), Pulsed (PT) Stepped Thermography (ST/SH), all of which have their own peculiarities and capabilities. A critical aspect concerns the overall lengthy time required for testing and analysis of thermographic data above all, for large structure where it is necessary a scanning approach. In this work, two algorithms based on the stepped thermography approach were investigated in quantitative way with the aim to optimizing the testing parameters and data analysis in terms of testing time and signal to noise ratio. In particular, several tests were carried out on a sample specimen with simulated defects and the well-established lock-in thermography technique has been used as comparison.

Keywords: GFRP; Stepped thermography; Lock-in thermography; Non-Destructive Testing.

1. Introduction

Composite materials, thanks to their high strength to weight ratio, are widely used for manufacturing large structures and components and in this regard, many examples can be found in different engineering fields from boating-yachting to aeronautical or aerospace. As clearly demonstrated in the literature [1], the presence of defects can dramatically change the strength of the structure and so, non-destructive techniques play a key role for estimating the residual strength of structures or components.

Many NDT techniques are currently used for defect detection in composites such as X-ray [2], ultrasound [3-6], shearography [7], vibration testing [8] and electrical potential technique [9] and in many applications a combination of them is necessary to identify different kinds of defects to quantify.

In the case of large structures, a rapid and easy inspection of components is required in order to reduce the time of the ordinary maintenance and thus to limit the costs. In this regard, it is very

important to develop automatic procedures and algorithms for data analysis in order to obtain more quickly the quantitative characterization of defects.

Stimulated thermography presents peculiarities suitable for investigation of large areas since it does not require the coupling with the component, is easily automatable and the testing time is relatively shorter with respect to other traditional well-established NDT techniques.

With regards of testing setup and data processing, the most diffused thermographic techniques for the non-destructive evaluation of composite materials are: Lock-in Thermography (LT), Pulsed (PT) and Stepped Thermography (ST/SH) [10-15]. All of them uses a surface or volumetric [16] heat source to stimulate with thermal waves the material in order to induce a heat flux in the material and analyse the temperature behaviour on the surface of the component. The main idea, common with all thermographic techniques is that a defect inducing different thermophysical local properties in the material, will induce also an anomaly in the thermal diffusion and then a different surface temperature of the component. In fact, these techniques look for areas of different thermal behaviour that can be correlated to a defect and that are typically dependent by different thermal-physical properties involved in the heat transmission phenomena such as the thermal conductivity, the specific heat at constant pressure and the density of material [10].

All the cited IR techniques have been used in various works and in many applications, demonstrating the ability of thermography to detect defects in CFRP and GFRP composite materials. In particular, these techniques are effective in the evaluation of interlaminar delaminations or debonds, and any kind of flaws parallel to the external surface.

Thermographic techniques have been used in combination with other NDT techniques to investigate defects in adhesively bonded components [17-21] while, many applications concern the investigation of composite material subjected to impact damage [12], [22] or dynamic loads [23], [24].

At the same time, different algorithms were developed in literature for analysing thermographic data and to detect defects. Different approaches were also used for lock-in thermography with the aim of reducing testing time. In particular, in the works of Palumbo [25] and Pitarresi [26], [27] a modulated heat source has been used for stimulating the specimen in a desired range of frequencies and extracting information about the simulated defects. A theoretical basis for describing this approach has been provided in the work of Mulaveesala et al., [28] where in a single test, hidden Teflon patches at various depths were detected. Algorithms associated with PT technique are summarized in [29] and here we can cite some of them, in particular: The Thermographic signal reconstruction [30], [31] and the Polynomial fitting [32].

In the work of Palumbo et al. [25] two parameters, the slope (m) and the linearity (R2) evaluated during the cooling semi-cycle of the first cycle of lock-in test, were taken into account to characterize defects behaviour. These parameters provide results in good agreement with the lock-in technique and seem capable to detect deeper defects even if with a higher level of noise. However, the results obtained in [25] with this approach were still not optimized in terms of testing time and signal to noise ratio. In this regard, in this work, the attention has been focused on the testing and processing parameters that affect the defect detection and estimation with the two parameters (m) and (R2). In particular, several tests have been carried out on a sample GFRP specimen with the aim to investigate both the effect of the heating time and the length of the cooling acquired sequences on the signal contrast.

Moreover, a quantitative data analysis has been performed by means of a semi-automatic algorithm, capable to discern defected from sound areas by means of two different approaches.

Finally, a quantitative comparison with the classic lock-in thermography technique is also provided.

2. Theory and proposed method

2.1 Stimulated Thermography: Pulsed and Lock-in thermography

Stimulated or active thermography needs an external heat source to stimulate the materials for inspection. Pulsed (PT) and Lock-in Thermography (LT) are the techniques most used in literature and they differ in the method used for heating the material.

Pulsed Thermography employs a short thermal stimulation to produce a thermal perturbation within the material [10]. The presence of a defect can be revealed by monitoring the surface temperature decay of the specimen. In fact, the defect appears as an area of different temperature with respect to a surrounding sound area and it produces an abnormal behaviour of the temperature decay curve.

As known [33], the presence of a defect at depth d alters the temperature decay at the surface $T(t)$, whose analytical formulation is:

$$T(t) = \frac{Q}{\sqrt{\pi \rho c k t}} \left[1 + 2 \sum_{n=1}^{\infty} R^n \exp\left(-n^2 \frac{d^2}{\alpha t} \right) \right] \tag{1}$$

where ρ is the mass density, c is the heat capacity, k is the thermal conductivity, α is the thermal diffusivity, Q is the source energy transferred to the surface and R is the reflection coefficient of the discontinuity.

Lock-in thermography is based on the generation of thermal waves inside the specimen, for example, by periodically exciting the specimen surface [10]. The resulting oscillating temperature field in the stationary regime can be recorded remotely through its thermal infrared emission by an IR camera. Thermal wave can be reconstructed by measuring temperature evolution over the specimen surface: by a suited algorithm, information about magnitude (A) and phase (φ) of the thermal wave can be obtained.
Phase data are relatively independent of local optical and infrared surface features and phase signal allows deeper penetration into the material than the analysis of the amplitude signal [10].

2.2 Stepped thermography: cooling analysis

As already explained in the section 2.1, under several hypotheses, the temperature trend can be described by the eq. 1, in the case of a Dirac pulse. Eq. 1, can be considered still valid also for finite short pulse duration. This approximation is still valid if the thermal wave does not reach the defect during the heating. So, a pulse duration of 5 seconds could be enough to consider eq. 1 still valid for a composite material but, the same pulse could be too long for high diffusivity materials such as aluminium.
Generally, in literature, the temperature rising process is studied to obtain information about the size and depth of defects [31]. The proposed approach is based on long heating pulsed and the investigation of the cooling curve. Unlike the pulsed approach, during the step heating, the thermal wave reaches the defect during the heating phase. This latter represents an obstacle at the normal heat diffusion so, the material before the defect will be warmer than the sound one. It follows that the temperature in defected area will be higher than in the sound one and then the defect will already appear during the heating (Figure 1). In similar way to the pulsed approach, the difference in temperature reached during the heating and the following cooling behaviour will depend on the different thermo-physical properties between defect and sound. In particular, the cooling of sound material follows the Newton's law [34] (exponential decreasing for homogeneous materials) while, defect area presents a different cooling rate and a departure from log-linearity with respect to the sound/homogenous material. In particular, the defect that is warmer than the sound material at the end of heating, exchanges heat for conduction and convention (in the case of flat bottom hole) more quickly than the sound. It follows a high cooling rate of defects with respect to the sound.
In Figure 1, a schematic representation of the pulsed and stepped approach is reported. In this regard, in this work, 2 indexes were used to describe the cooling behaviour of the material: the slope (m) and the R2. These latter can be used both for pulsed and stepped thermography. The R2

parameter calculation is implemented in the software IRTA [35]. In the case of a simple linear regression, R2 equals the square of the Pearson correlation coefficient between the observed and predicted data values of the dependent variable [36].

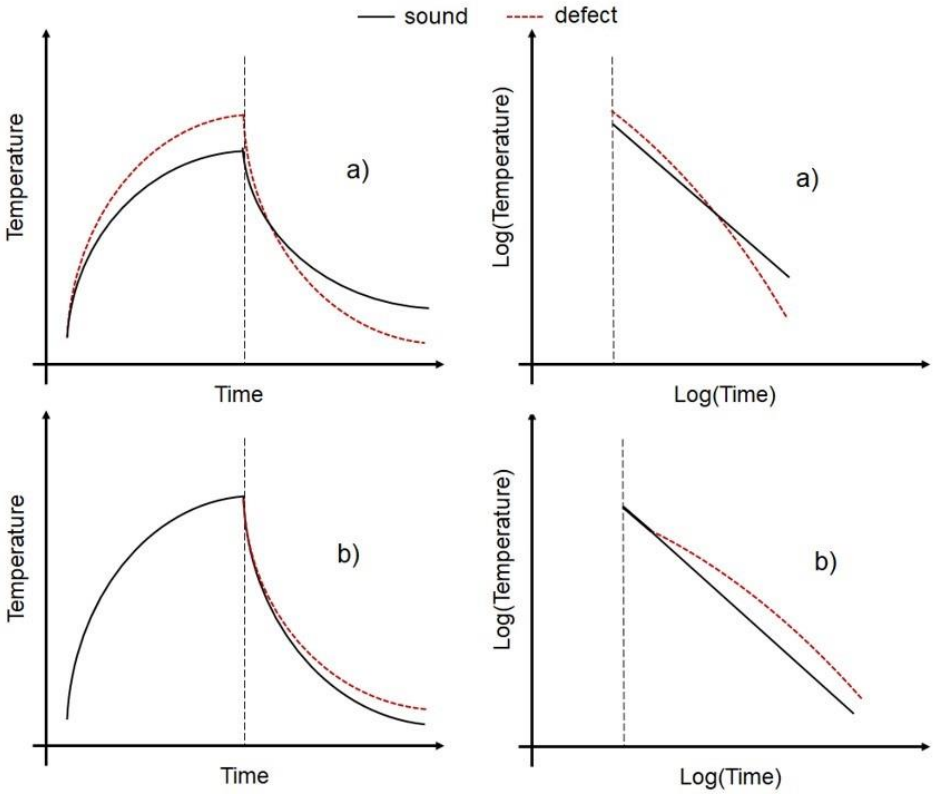

Figure 1. Temperature trend in defect and sound area, a) Stepped approach, b) Pulsed approach

3. Material and set-up

A specimen consisting in a plate with simulated defects was manufactured by means of the vacuum infusion resin process. An epoxy-type (i.e. EC 157 by ELANTAS) resin was employed, reinforced with a double layer of quadriaxial glass fibre of the type 0°/+45°/90°/-45°, Figure 2. Dimensions and depth of defects are reported in Figure 1. Thermography tests were performed by IR camera FLIR A655sc with thermal sensitivity (NETD) < 30 mK and based on a micro bolometer detector with 640×480 pixels.

The set-up used is shown in Figure 2. Two halogen lamps with a power of 500 W were controlled by MultiDES® system in order to heat specimens with a series of square waves. The geometrical resolution obtained is 0.65 mm/pixel.

Thermal data were processed by IRTA® software in order to obtain amplitude and phase images from lock-in tests, slope m and R2 from the analysis of the cooling curve (Stepped Thermography). IRTA algorithms [35] for lock-in take into account the thermal transient in the very first cycles. So, there is no need to reach stationary behaviour of the thermal response of the material to the excitation source.

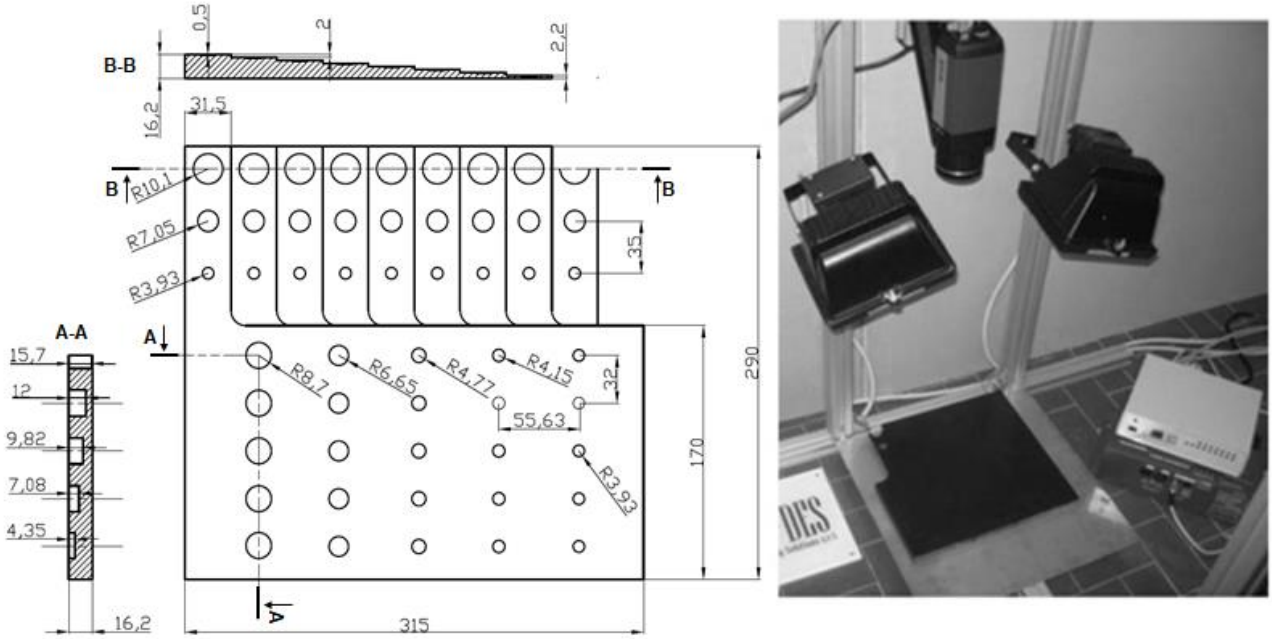

Figure 2. GFRP specimen and experimental set-up

4. Data analysis

4.1 Lock-in thermography analysis

In this work, a modulated square wave has been used as a heat source in order to reduce the testing time. In fact, as demonstrated in other works [25-27], the thermal response of material contains information about higher frequencies proportional to the main frequency. By decomposing the thermal response in time domain as the sum of a singular sinusoidal wave, we can write:

$$T_m(t) = a + bt + \sum_{n=1}^{\infty} \Delta T_n \sin(n\omega t + \varphi_n) \qquad \text{n=1,3,5,7,……..} \tag{2}$$

where t is the time, a and b are two constants used to model the average temperature growth of the material, ω is the modulated frequency of the main harmonic (first Fourier component), ΔTn and φn are the amplitude and the phase of n-th Fourier component.

In this work, all the constants were obtained through a least-square fit method by imposing the model of Eq. (2) to the thermal signal of each pixel and by considering the terms up to n=5. In this way we can write:

$$T_m(t) = a + bt + \Delta T_1 \sin(\omega t + \varphi_1) + \Delta T_3 \sin(3\omega t + \varphi_3) + \Delta T_5 \sin(5\omega t + \varphi_5) \quad (3)$$

Equation 3 allows us to obtain information about the amplitude and phase signal of high order excitation frequencies with respect to the main by a single lock-in test.

4.2 Data analysis: proposed algorithm and signal contrast evaluation

Several tests have been carried out as shown in Table 1 and Table 2. In particular, the cooling analysis of ST technique (slope and R2) has been performed by considering different cooling time intervals. Each interval has been expressed as % of the total frames acquired during the cooling phase (cooling time) by considering a fixed start frame, coincident with the frame where the maximum temperature is reached. As it can be observed from Table 2, it has been considered a constant fixed ratio of 7:1 between the cooling and heating time intervals.

Table 1.Parameters used for LT tests (acquired 100 frames/cycle).

Modulation Period (s)	Modulation Frequency (Hz)	Heat source	Number of cycles	Harmonics (Hz)	
48	0.021	square	3	0.021; 0.062; 0.105	I; III; V;
72	0.014	square	3	0.014; 0.042; 0.069	I; III; V;
80	0.013	square	3	0.013; 0.038; 0.063	I; III; V;
120	0.008	square	3	0.008; 0.025; 0.042	I; III; V;
240	0.004	square	3	0.004; 0.013; 0.021	I; III; V;
360	0.003	square	3	0.003; 0.008; 0.014	I; III; V;

450	0.002	square	3	0.002; 0.007; 0.011	I; III; V;

Table 2.Parameters used for ST tests.

Heating time (s)	Cooling time (s)	Sample rate (frames/s)	Analysis: % of total frames
24	168	6	5, 10, 15, 20, 30, 40, 50, 60, 70, 80, 90, 100
36	252	4	
40	280	4	
60	420	2	
120	840	1	
180	1260	1	
225	1575	1	

The combination of test parameters generated a series of results in image format each one containing 25 virtually significant indications (simulated defects). In this regard, a semi-automatic algorithm has been developed for analysing the huge number of data.

It is worth noting that the aim of this work is the comparison among data processing methods. So, the proposed algorithm starts from the knowledge of the defects position (Figure 3) and performs the quantitative analysis in automatic way. In particular, the Standard Deviation (SD) of the signal has been used to discern defected areas from sound ones.

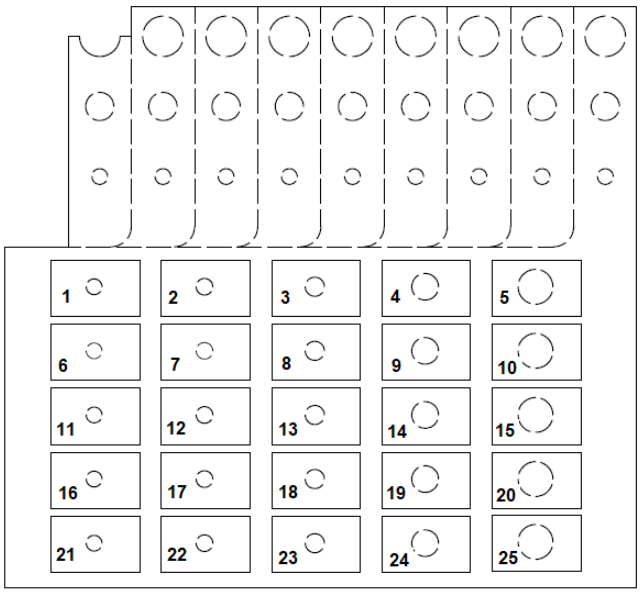

Figure 3. Scheme of the investigation areas, each one including one defect

Figure 3 shows a scheme of the investigation areas used for the analysis of each defect. This approach allows us to discern in automatic way, defect from sound areas. Figure 4 shows clearly as SD allows for the defect peak determination in two different cases where the signal of defected pixels is first higher and then lower than the sound ones. The defect peak position is obtained from the intersection between the maximum SD value of the signal measured along the rows and columns of the analysed area. The sound area has been automatically selected by considering the SD values below one half of the SD peak amplitude in each investigation area.

As example, Figure 5 shows for the area around the defect n.2, the assessment of the sound and the defected area (36 sec of step heating, 10% of cooling frames) (slope parameter).

The generic signal contrast ΔS/SD has been calculated as follow:

$$\frac{\Delta S}{SD} = \frac{mean(A_d) - mean(A_s)}{SD(A_s)} \tag{4}$$

where Ad represents the defected area determined by considering an area of 3x3 pixels centred on peak value of the signal SD and As the sound are obtained as previous exposed.

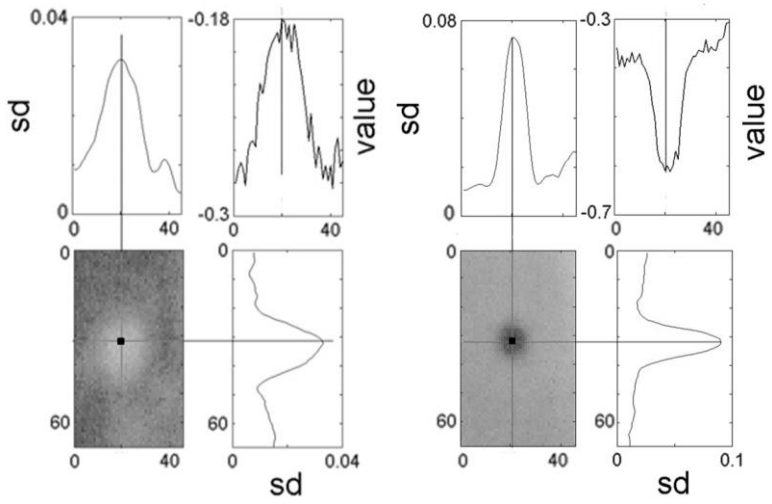

Figure 4. Automatic peak defect detection: defect n.2 (on the right) defect n.9 (on the left) both in 36 sec step heating, 10% of cooling frames, not filtered slope map)

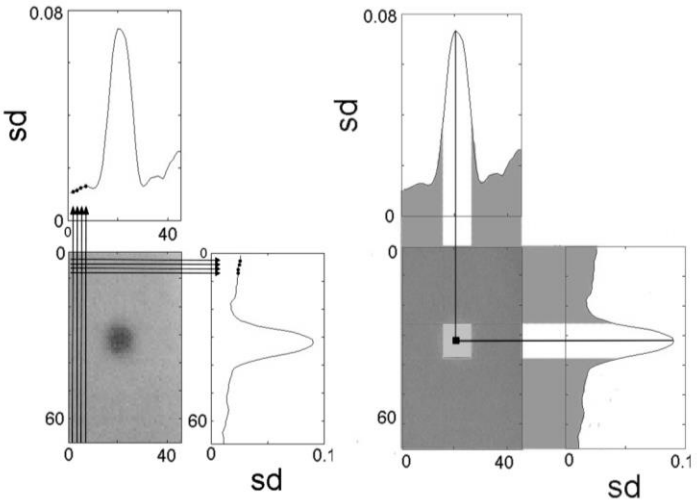

a) b)

Figure 5. a) SD profiles and b) defect and sound area detected (defect n.2, 36 sec, 10% of cooling frames) (slope parameter)

Summarizing, the following steps of proposed algorithm allow for the determination of the signal contrast:

Step.1: Creating of investigation areas:

1. Obtaining slope m and R2 and phase images from IRTA software;
2. Filtering each image by means of the median filter;
3. Extracting ROI from images in order to obtain investigation areas;

Step.2: Calculating the signal contrast of defects in each investigation area:

1. Selecting the investigation area;
2. Creating two vectors with data standard deviation values of each row and column;
3. Searching for maximum values of each vector in point 2 in order to obtain signal peak coordinates;
4. Giving a zero-signal contrast value if peak coordinates are beyond nominal defect area;
5. Calculating the mean value of the signal defect value by considering a 3x3 matrix centred on the peak coordinates;
6. Searching for rows and columns that present a standard deviation value below the imposed threshold value (one half of the SD peak amplitude);
7. Giving a zero-signal contrast value if the sound area As is less than 30% of the total investigation area;

8. Calculating the mean and the standard deviation of sound pixel;
9. Calculating the signal contrast;

Figure 6 contains a flow chart of the Step1 of the proposed algorithm while Figure 7 shows Step 2.

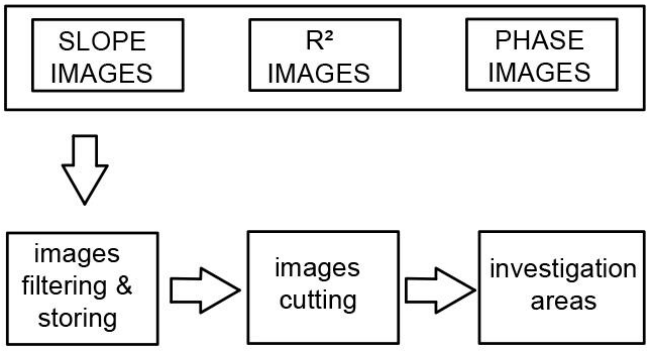

Figure 6. Steps 1 of the proposed algorithm for the analysis of thermographic data

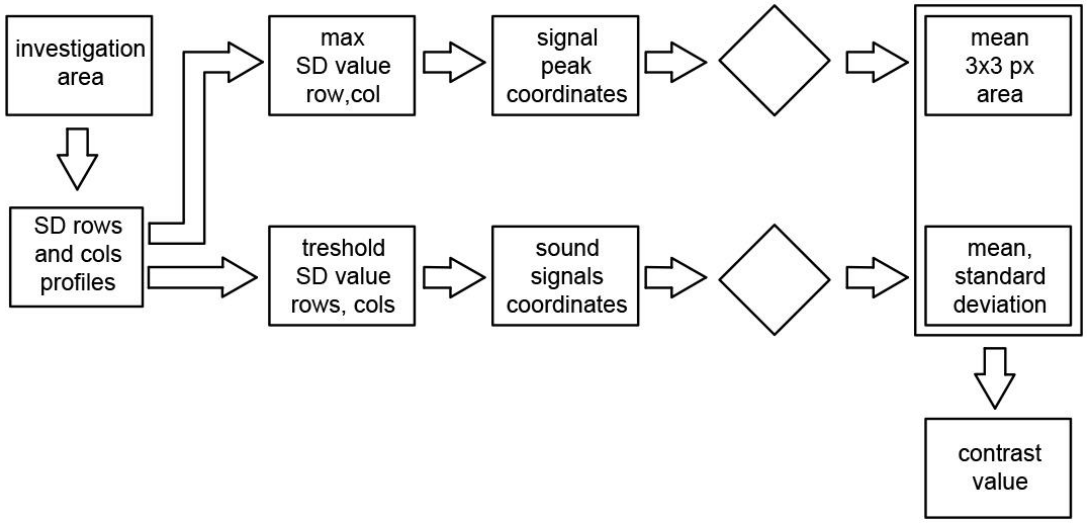

Figure 7. Steps 2 of the proposed algorithm for the analysis of thermographic data

In Figure 3 is shown a preview of the investigation areas chosen for each defect.
Points 4 and 7 of the proposed procedure of analysis represent two discarding criteria to avoid false positives and too low values of the signal contrast. Indeed, if few data are selected for As, a high value of SD is obtained in sound area with a consequent low value of ΔS/SD.

4.3 Data analysis: quantitative evaluation of defects dimension

Last step of procedure is the quantitative analysis, carried out in order to compare the two different techniques used in this work (Lock-in and Stepped thermography) by means of a decision threshold

values criterion. In particular, two different approaches have been used for the quantitative analysis. In the first one, the threshold criterion approach has been applied by considering the signal output of each algorithm while, the second considers the SD values obtained from the SD profiles. In this regard, the threshold value Th has been defined considering the following equation for the first approach:

$$Th = \alpha[mean(A_d) - mean(A_s)] + mean(A_s) \tag{5}$$

and for the second one:

$$Th = \alpha[\max(SD) - \min(SD)] + \min(SD) \tag{6}$$

where the parameter α has values between 0.05 and 0.95 with step 0.05.
The application of eq. (5) and (6) to all results in terms of phase images for lock-in technique and R2 and m for stepped technique, allows for obtaining binary images. From these images, it is possible to evaluate the defect area by summing the pixels with 1 value.
The measured defect area (MDA) has been compared with nominal defect area (NDA) in order to obtain the error of estimated defect area (AER) for each α value:

$$AER\% = \left|1 - \frac{MDA}{NDA}\right| * 100 \tag{7}$$

Also, in this case, two discarding criteria have been used to avoid false positives. The first regards the number of pixels with 1 value considered in the binary image. Only the pixels included in a circular area centred and equal to the 150% of the nominal defect area (NDA) have been considered in MDA evaluation. This procedure allows us to avoid spurious pixels that assume 1 value within the ROI.
Hence, it has been considered a hit a result in term of MDA area with an error (AER%) below 10%. In other words, only the alpha values that provide an AER%≤10% were considered for the analysis. The choice of this threshold of 10% error is arbitrary but seemed to be reasonable considering the inherent error in defect dimension determination typical of industrial NDT techniques.
Summarizing, the following procedure has been adopted:

1. Introducing a threshold parameter (α) varying from 0.05 to 0.95 with step of 0.05;

2. Estimating the defect area as function of each α;

3. Comparing each estimated area with relative nominal area and calculating the estimation error;

4. Successfully considering all cases in which the error is less than 10%;

Figures 8 and 9 resume the procedure used for quantitative analysis while in Figure 10 an example of procedure is shown for defect n.2 (225 sec step heating, 5% of cooling frames) (slope parameter).

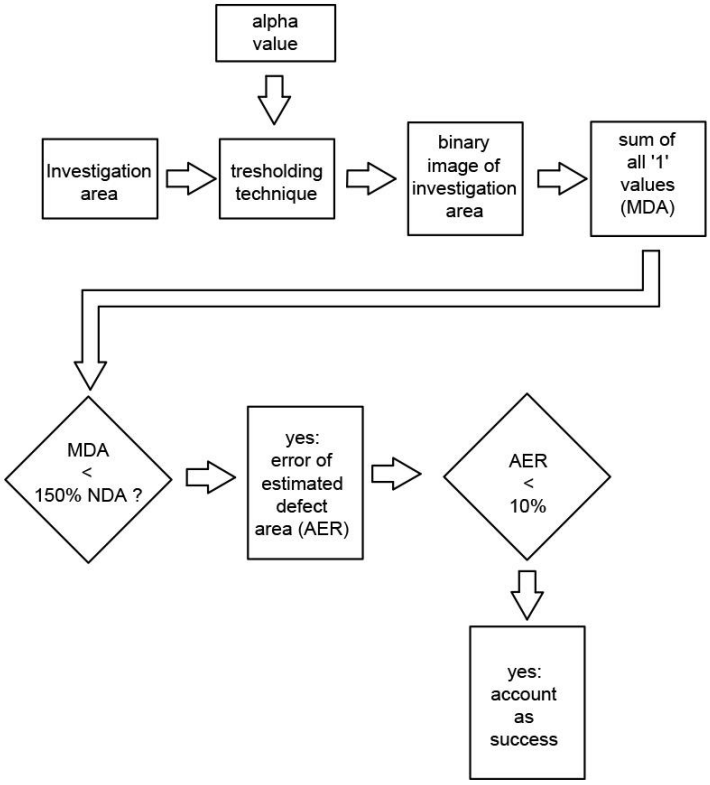

Figure 8. Flow chart for first approach procedure for defect size assessment

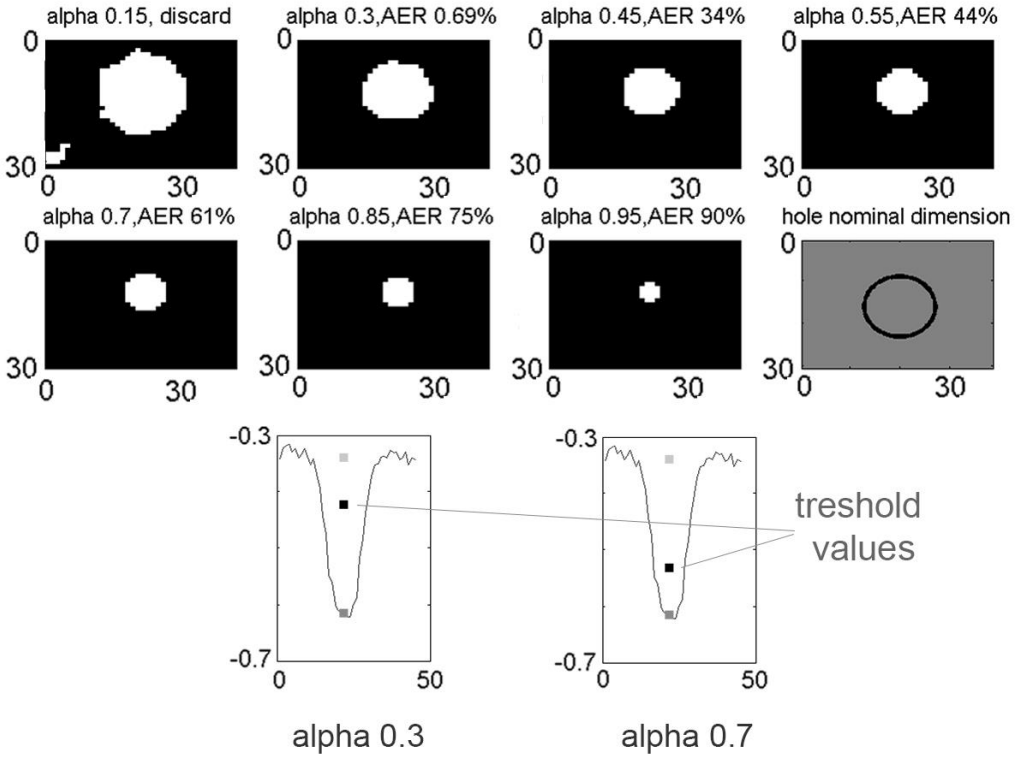

Figure 9. Influence of alpha parameter on quantitative analysis for defect n.2 (225 sec, 5% of cooling frames), first approach, (slope parameter)

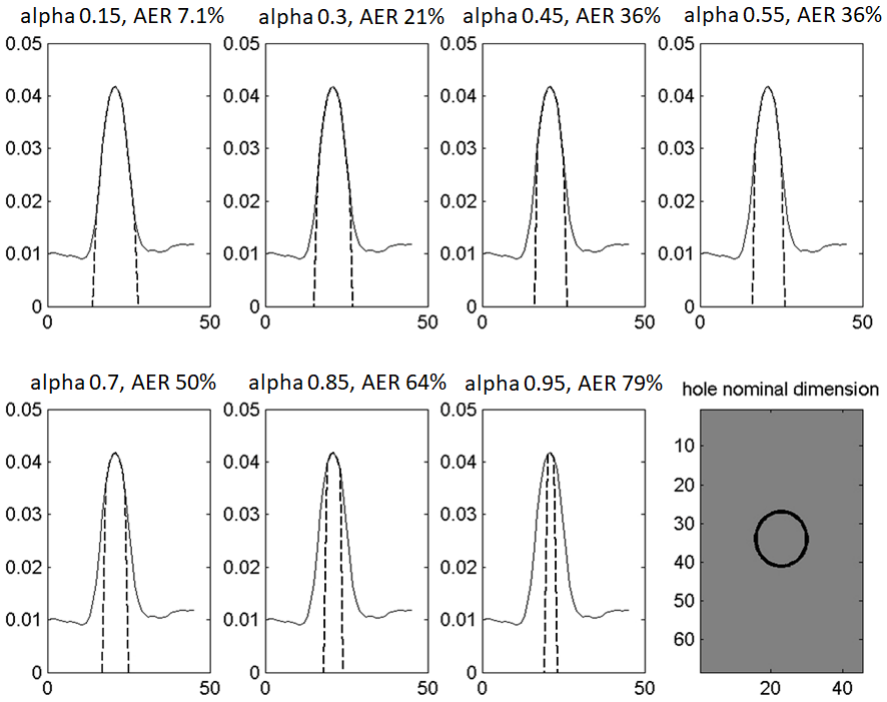

Figure 10. Influence of alpha parameter on quantitative analysis for defect n.2 (225 sec, 5% of cooling frames), second approach, (slope parameter)

5. Results and discussion

Stepped thermographic technique involves a step heating stimulation and the investigation of the thermal signal during both the heating and the cooling over time. Other works in literature [25] demonstrated the potential of the two parameters m (slope) and R2 in evaluating defects in composite material. However, the test parameters and their optimization have not been deeply investigated yet.

In this work, the relation between the number of selected cooling frames and the thermal contrast has been investigated both for the slope (m) and the R2 parameter and a comparison with the lock-in thermography technique is provided.

Stepped images have been computed in IRTA fixing the first cooling frame in correspondence of the maximum temperature frame and setting last frame as a percentage value of the total frame of the cooling sequence.

In Figure 11 is shown, as example, the cooling curve of the sound area obtained for a heating time of 225 seconds. In particular, it is represented the influence of the number of frames (sequence length) on the values of slope m and R2. In the first case, in which the total sequence is considered, a lower value of the R2 and a higher value of the m are obtained with respect to the last case. This example demonstrates as the signal, its contrast and then the probability to detect a defect, can be influenced by the number of frames chosen for the analysis. As just said, many sequences have been tested in order to describe the influence of this parameter on contrast values.

5.1 Stepped thermography: slope parameter (m)

Figure 12 shows four slope maps obtained for the same heating time (24 sec) and four different number of frames expressed as % of the total number of frames. As expected, it is clearly seen the influence of the considered number of frames on the signal contrast.

Figure 13 shows the signal contrast values against frame percentage for 24 seconds of heating and for all the defects of specimen. It is clearly visible that, the maximum signal contrast is reached within 40% of cooling sequence, except for defect n°1. Also, it appears that contrast values of first row of defects are bigger than the second row and also, they have different sign. The sign of the signal contrast depends on the heating time and the % of frames considered for the analysis. As already explained in the theory section, thermal waves can reach the defect during the heating (Figure 1, Stepped approach). In this case, the defect will present a higher slope than base material and then the sign of the signal contrast will be negative (the defect exchanges heat for conduction and convention more quickly than the sound). On the contrary, for the pulsed approach, the defect

will present a cooling rate lower than the sound material and then a positive signal contrast. Moreover, the signal of the contrast changes also as function of the number of frames considered for the analysis. In fact, above all for the heating time of 60 s, a change in sign can be observed (Figure 14). In this case the cooling behaviour of the defect presents a mixed mode between the stepped and pulsed approach. Moreover, this behaviour could be used for discerning the depth of defects. In fact, in this case, the first raw of defects can be considered representative of sub-superficial defects characterized by higher temperatures than sound material and then by a more rapidly cooling phase.

Big contrast difference between first and second defects row is due to their thickness difference, 0.5 mm for the first row and 4.2 mm for the second one.

Finally, it seems that the diameter has less influence on the contrast as depth, but its influences cannot be negligible, since the minimum diameter detectable is 7.8 mm for the first row, 8.3 mm for the second row and 17 mm for the third one.

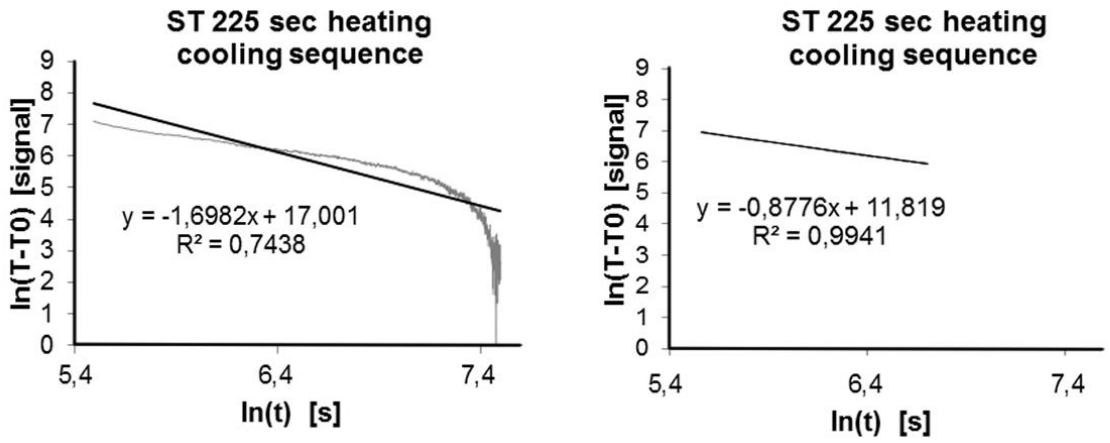

a) b)

Figure 11. Effect of number of frame on m and R2 values by means of the linear least square analysis

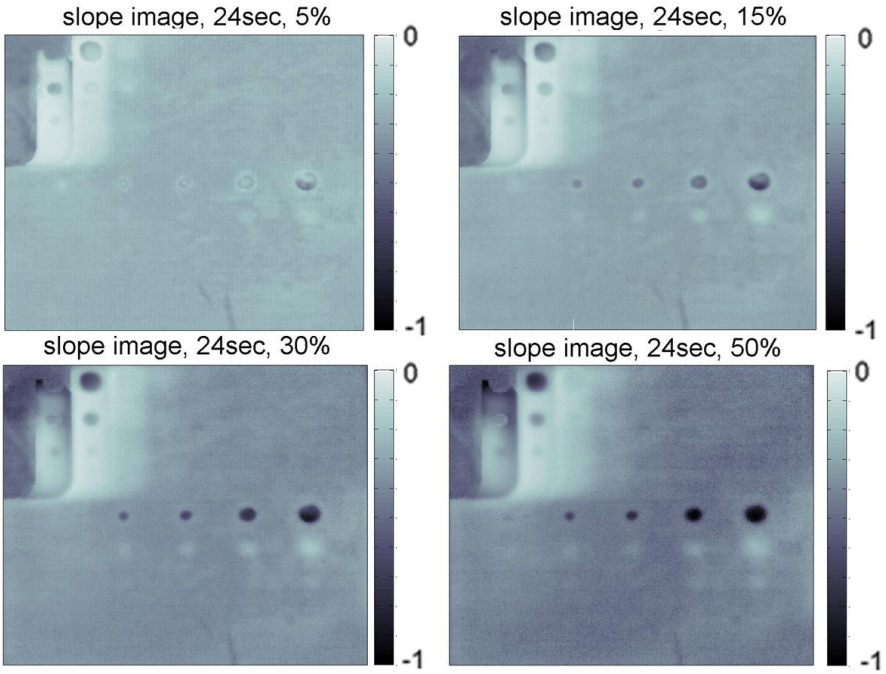

Figure 12. Slope images: comparison among different images obtained by considering different values of the % of frames

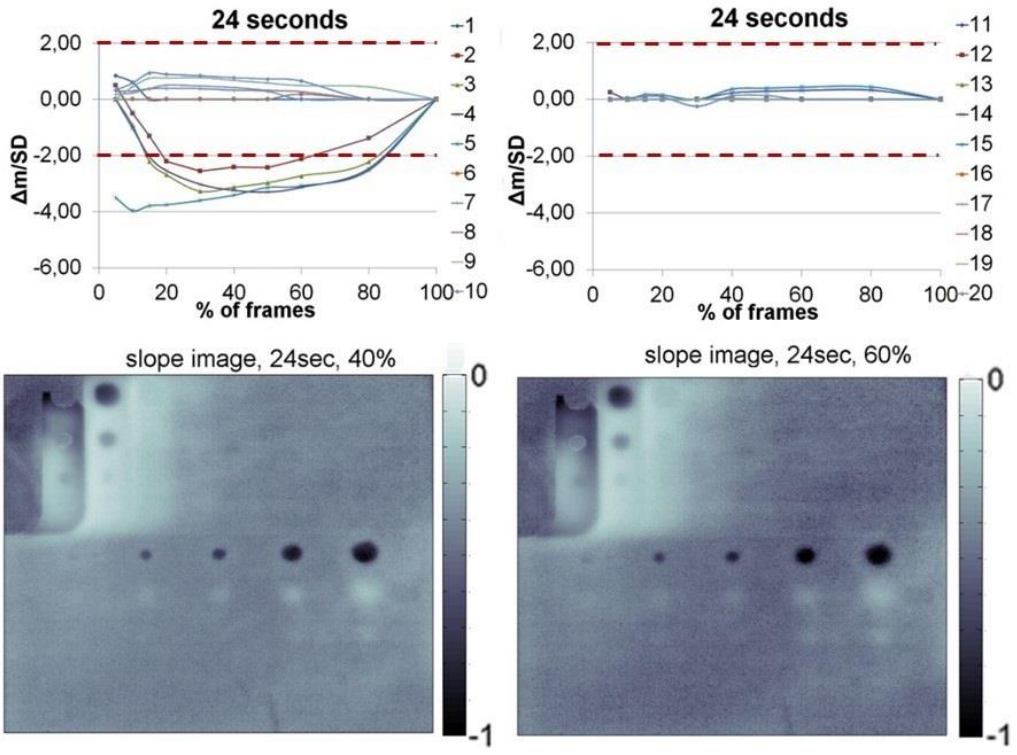

Figure 13. Slope contrast vs. % of frames and slope images obtained for the 40 % and 60% of frames (heating duration: 24 seconds)

Figure 14, relative to 60 seconds of the heating time, shows for the first row of defects a signal contrast comparable with the one obtained with a heating of 24 second. The maximum value of the

signal contrast is obtained for lower values of % of frames and for defects placed at 4.2 mm (second row) a signal contrast close to zero was obtained within the range 30%-50% of frames. Then the signal changes in sign and increases in the range 60%-90%. In other words, the range 30%-50% represents a range in which defects of the second raw are not detectable. As it is shown in Table 3 and in Figure 15, this "blind zone", for defects placed at 4.2 mm, appear for each adopted heating time and seems move towards earlier frames as heating time increases. This zone could be used for defect depth estimation as well as the blind frequency is used for the Pulsed Phase Thermography technique [10]. Further works will investigate the relation between blind zones and depth of defect.

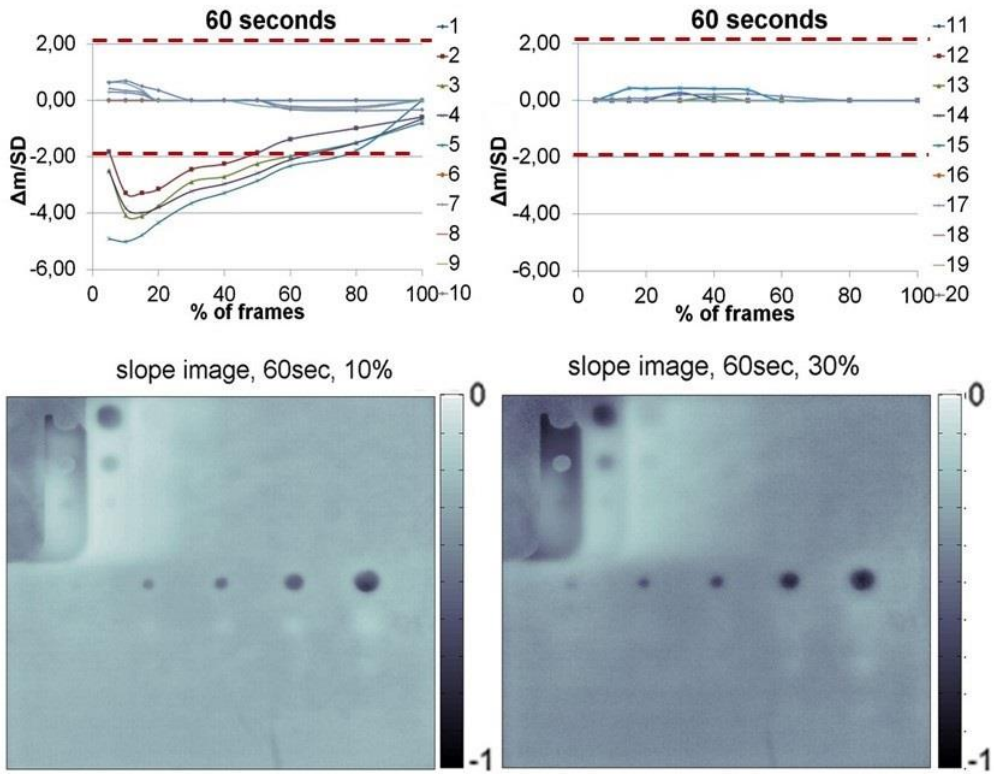

Figure 14. Slope contrast vs. % of frames and slope images obtained for the 10 % and 30% of frames (heating duration: 60 seconds)

Table 3. Blind range in terms of % of frames obtained in correspondence of different heating time related to the second row of defects (depth 4.2 mm, slope parameter)

Heating time (s)	Blind range (% of frames)
24	0%
36	5% - 10%
40	10% - 20%
60	30% - 50%

120	10% - 20%
180	5% - 10%
225	0%

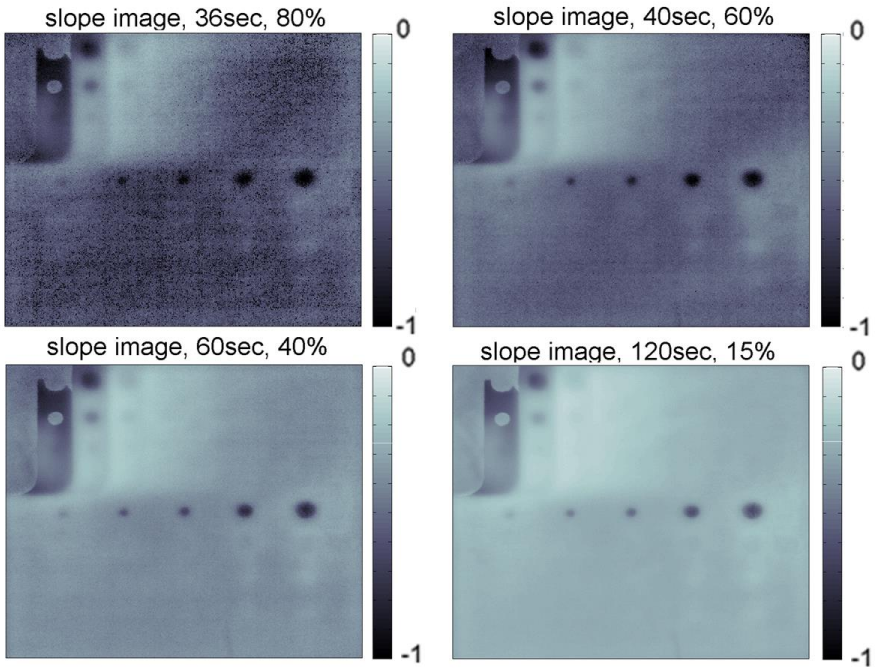

Figure 15. Slope images in correspondence of the blind range in term of % of frames for the second row of defects

As expected, the signal contrast of the second and third row of defects increases as the heating time increase (Figure 16). It is interesting to notice as, for these defects, the zone of the maximum contrast is placed between 20-60% of total frames.

Dotted red lines reported in all figures represent two reference values above of which the signal contrast could be considered significant with respect to the noise. This latter has been fixed for all tests equal to two times the Standard Deviation in the sound areas.

Slope parameter presents significant values of the signal contrast only for the first row of defect placed to 0.5 mm.

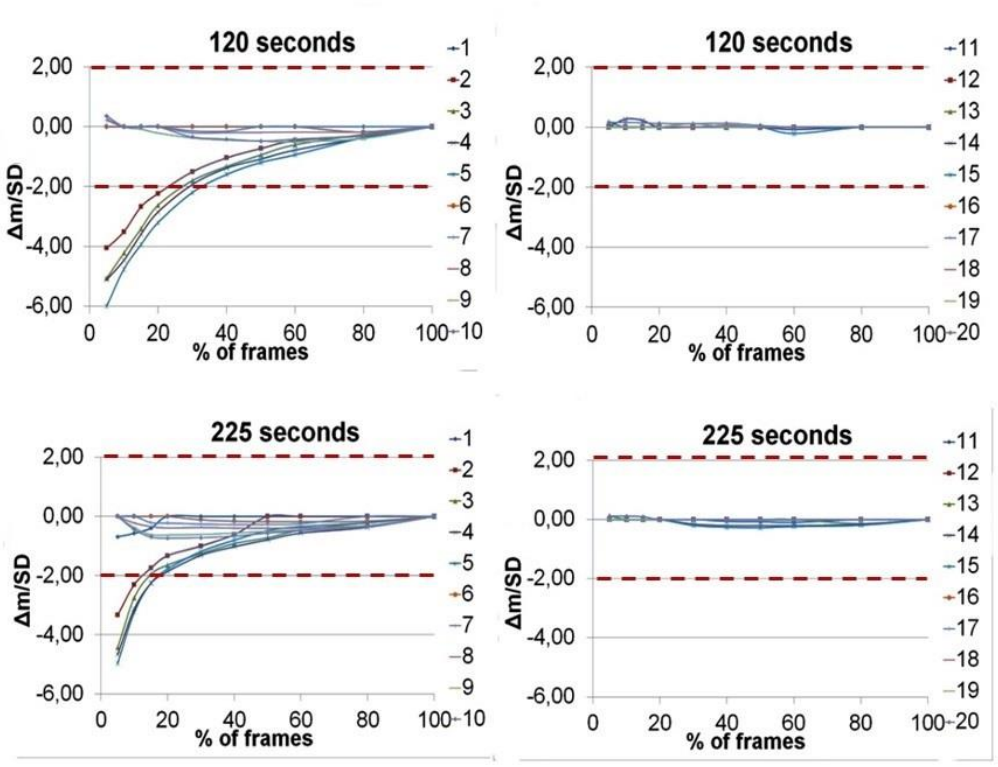

Figure 16. Slope contrast against % of frames for 120 and 225 seconds of heating time.

5.2 Stepped thermography: linearity parameter (R^2)

As already exposed in previous sections, R2 is a measure of linearity of the cooling curve in the log-log diagram.

Contrast values are comparable with the slope ones and R2 maps are affected by a lower signal to noise ratio. Indeed, deeper defects present contrast values higher or very close to the reference values (2*SD).

Interesting consideration it can be done analysing the R2 maps and the particular geometry of indication in presence of defects. In fact, as shown in Figure 17 in which the signal trend is reported along a profile through the defect n.3, it is possible to observe a double signal change concavity in proximity of the edges of the defect. Furthermore, in Figure 18 and Figure 19, first row defects give an indication that is quite annular. These evidences should be matter of further investigation, but these results show as R2 is capable to detect the edges of defects better than the slope parameter. However, the proposed procedure used for evaluating in semi-automatic way the defect size, does not consider these kinds of defects because of the double concavity of SD profiles, as seen in Figure 17.

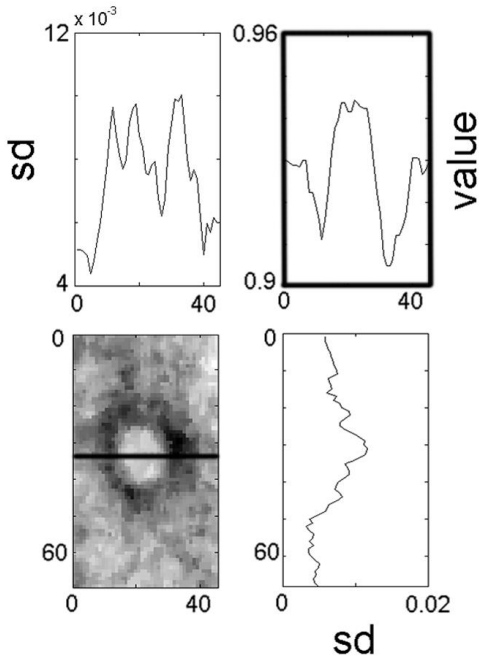

Figure 17. R^2 image of defect n. 3 (36 sec, 40% of frames sequence)

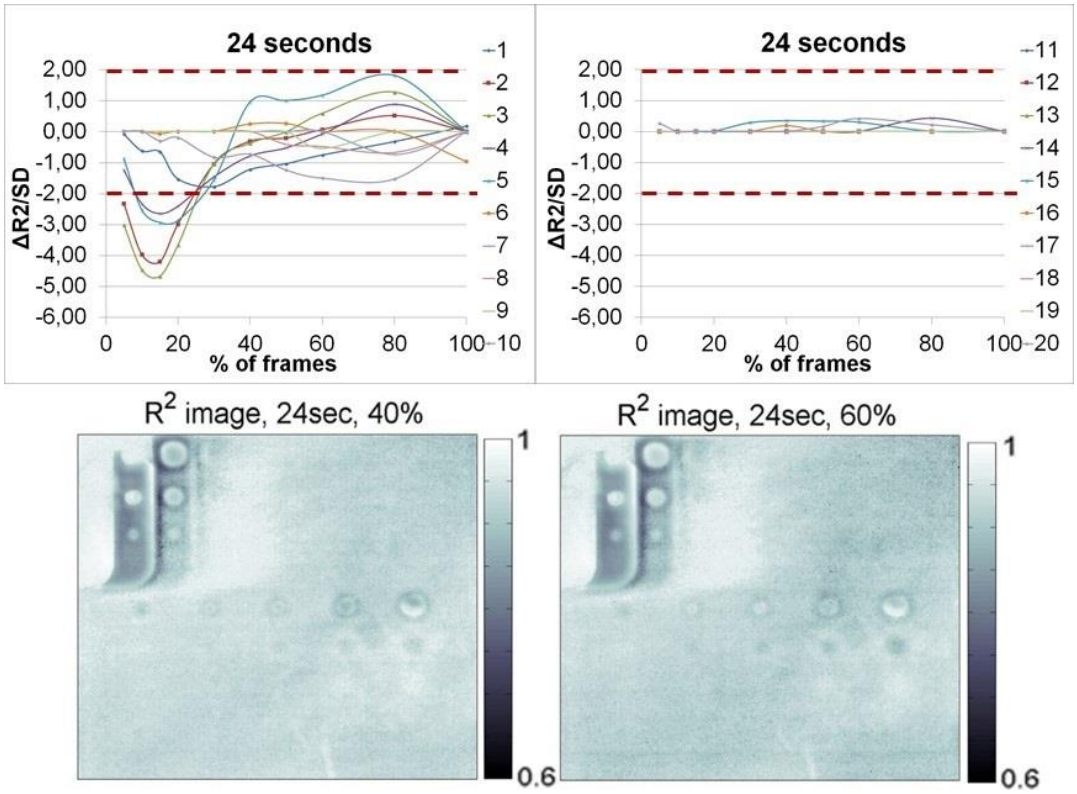

Figure 18. R^2 contrast vs. % of frames and R^2 images obtained for the 40 % and 60% of frames (heating duration: 24 seconds)

The signal contrast variation has, in this case, a more irregular trend and seems to be more sensible than slope to the % frames used for the analysis. High contrast values are also reached for high values of % frames (high cooling time) and for the heating times of 120 and 225 s significant signal

contrast are obtained for defects 14, 15, 20 of the third and fourth raw, Figure 18, Figure 19, Figure 20. In this regard, R2 shows a good sensibility for deeper defects. Also, it is interesting the behaviour of the first raw of defects characterized by high values of R2 close to 1. As showed in Figure 21, for 60 seconds of heating time (image on top right represents thermal frame when maximum temperature is reached), shallower defects have been subjected to overheating. So, they show a faster cooling than sound zone. Faster cooling led to a cooling law so quickly that could match a linear behaviour in earlier frames. In particular, by considering earlier cooling frames for defects n. 5, a R2 value closer to 1 than sound is obtained.

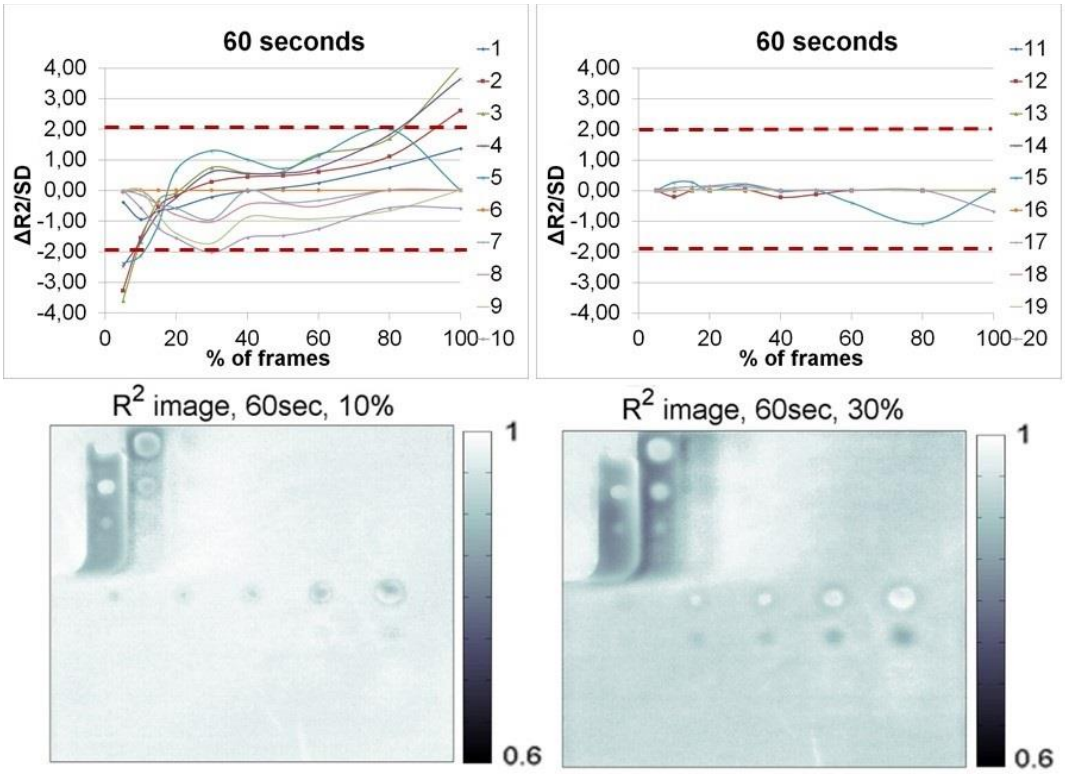

Figure 19. R^2 contrast % of frames and R^2 images obtained for the 10 % and 30% of frames (heating duration: 60 seconds)

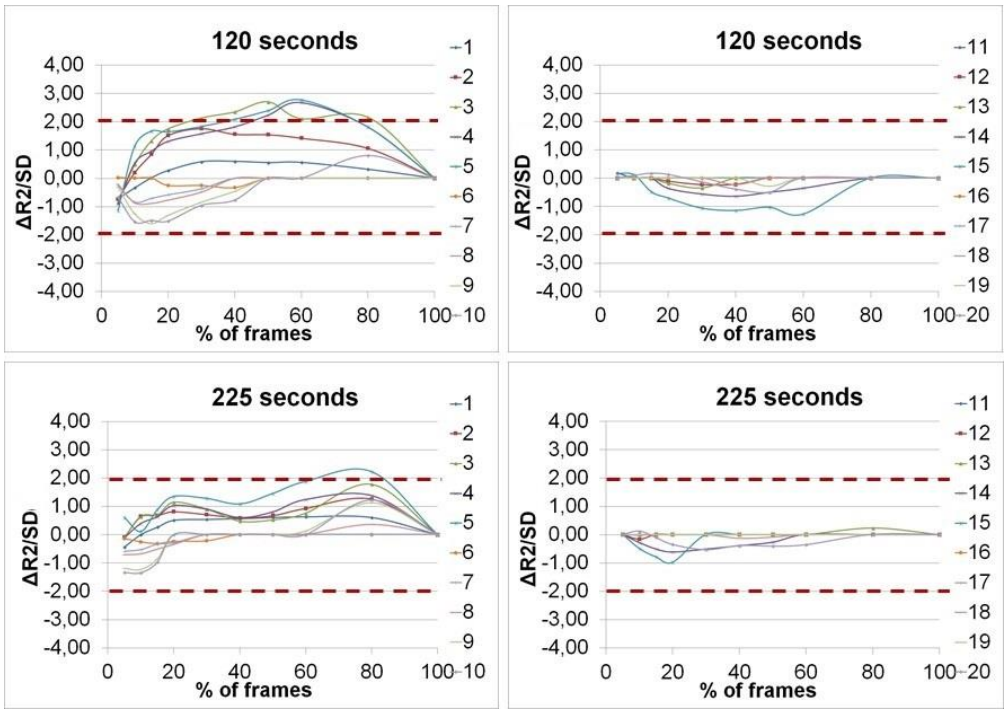

Figure 20. R^2 contrast vs. % of frames for 120 and 225 seconds of heating

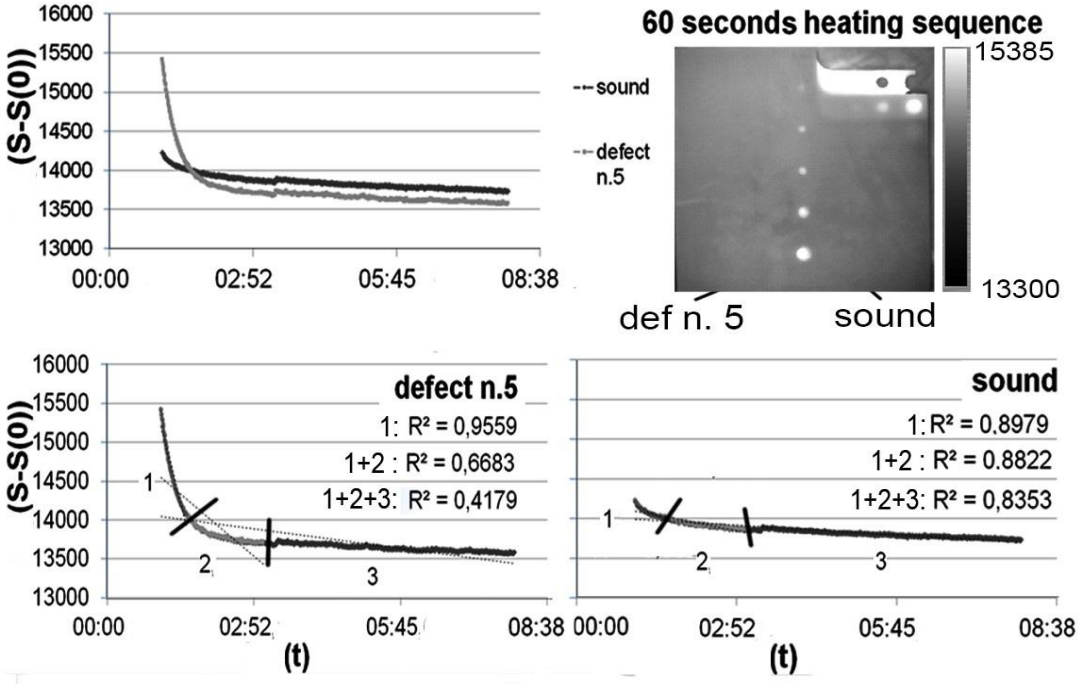

Figure 21. Influence of the % of frames (different time interval) on R2 assessment. (In these graphs S is thermographic signal from IR camera and S(0) thermographic signal at t=0 sec; image on top right is thermal frame at max temperature, expressed as IR camera signal unit);

5.3 Quantitative analysis and comparison with lock-in thermography

Phase contrast values are plotted against modulated period in Figure 22. It can be seen as lock-in analysis provides a signal contrast greater than R2 and m. However, the capability to detect deeper defects depends on the modulated periods and then the testing time increases as the depth of the investigated defects. Also, in this case a blind modulated period is present at 100 s for defects placed at the same depth (first row). Defect diameter has less influences on contrast, particularly at lower modulated periods.

Figure 23, Figure 24 and Figure 25 show bar charts where are summarized the successful cases in quantitative analysis. These results were obtained by considering all data (84 maps for R2 and m and 21 for phase signal) and all defects. As it is described in section 4, the successful/positive matches are obtained for an error below 10% with respect to the nominal defect and are expressed as % values with respect to the total number of cases.

It is interesting to underline as the second approach (proposed in this work) gives back more positive match results than the first one (used in literature [37], [38]).

Figure 25 shows as for lock-in thermography the positive matches are quite higher in number than stepped method. This behaviour, as expected, is due to the higher values of signal contrast with respect to the stepped technique.

In each case, it is shown as the best α value (for which the higher number of positive matches is obtained) depends on the approach used for defining the signal contrast. In particular, obtained values are in each case below 0.5 that is generally used in literature for the quantitative analysis of thermographic data [37], [38]. Moreover, with the first approach and above all, for the slope and phase parameters, different values of alpha are needed to quantify the major number of defects to different depths. On the contrary, indeed, the second approach allows to quantify defects to all depths with only one alpha value.

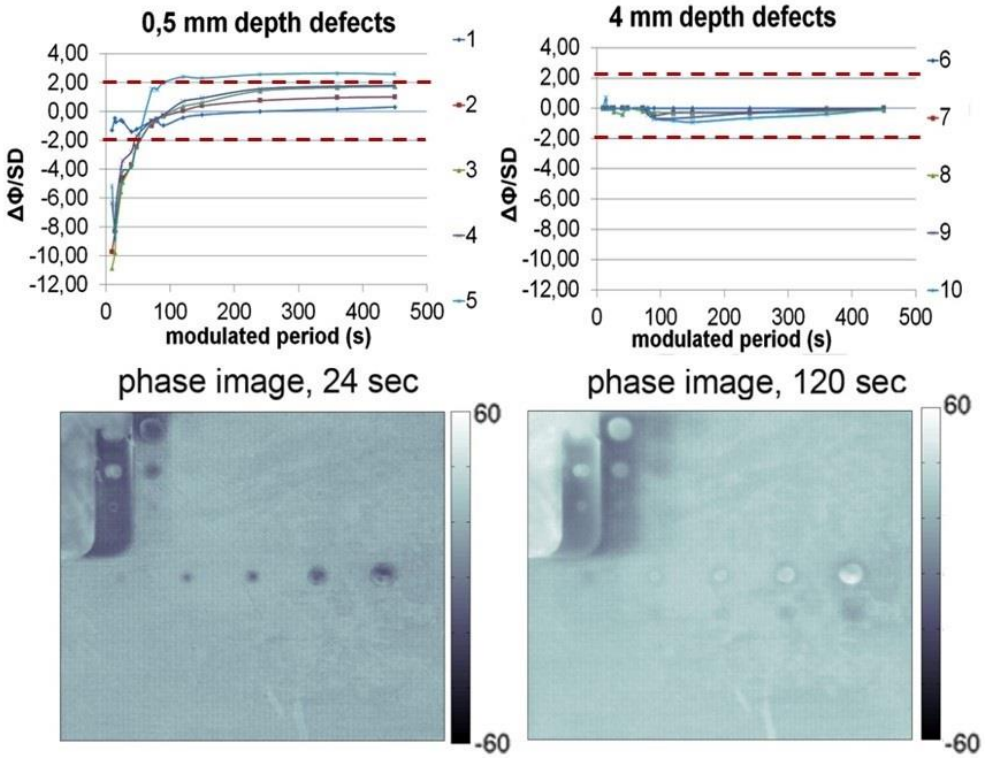

Figure 22. Phase contrast against modulated period.

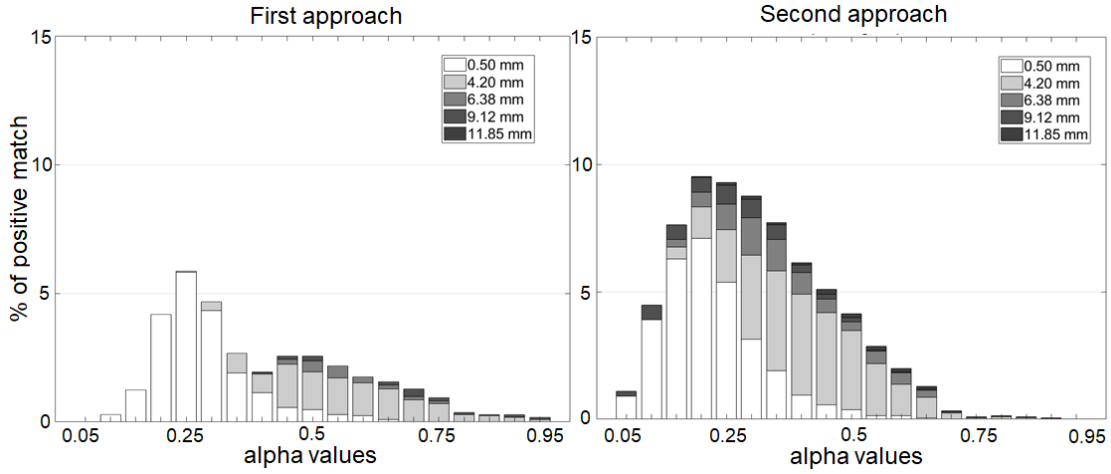

Figure 23. Positive matches against alpha values for both the first and the second approach (slope)

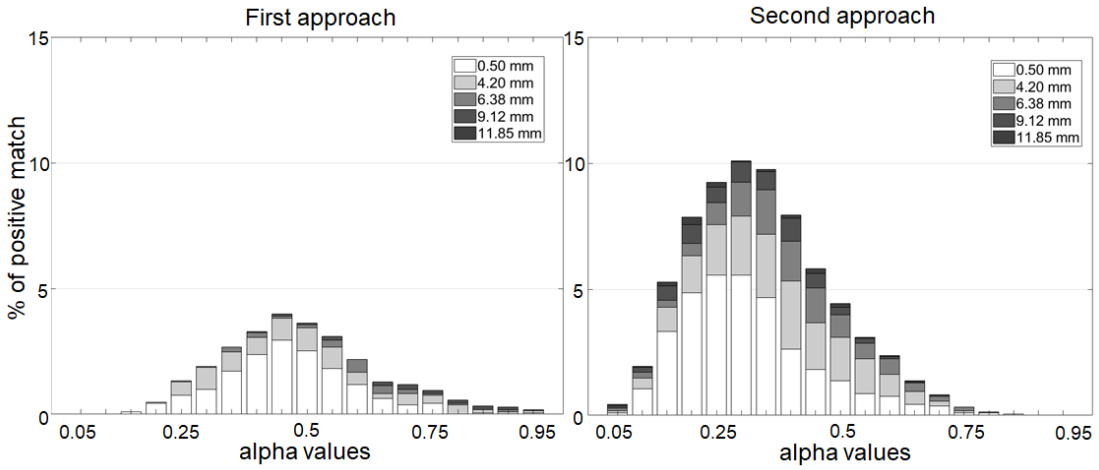

Figure 24. Positive matches against alpha values for both the first and the second approach (R^2)

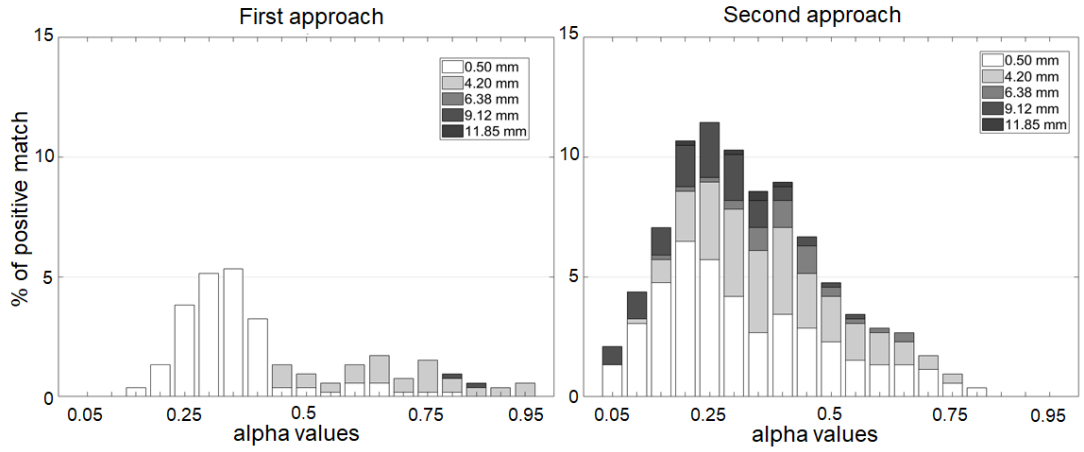

Figure 25. Positive matches against alpha values for both the first and the second approach (phase)

6. Conclusions

In this work, two different parameters, slope (m) and R2, obtained by analysing thermographic data derived by stepped thermography tests were investigated.

Different tests were carried out on a GFRP specimen with flat bottom holes with the aim to optimize defects detection in terms of testing time and signal to noise ratio. In particular, it has been investigated the effect on the signal contrast produced by changing both the heating time and the % of frames considered for cooling analysis.

A quantitative analysis based on the signal contrast has been carried out for comparing the proposed analysis with the well-established lock-in thermography technique.

The main results can be summarized as follow:

- As expected, the signal contrast for both parameters depends on both the defect diameter and depth.
- Slope (m) presents a signal contrast with a regular dependence from the % of frames and changes in sign in correspondence of a suitable range of % of frames. This blind range could be used for estimating defects depth. For different heating times, the analysis of 40 % of frames seems sufficient to detect defects at different depths.
- R2 gives higher values of the signal contrast with respect to m and seems capable of detect the edges of defects. However, R2 presents an irregular dependence from the % of frames in correspondence of different heating times.
- Phase data (lock-in thermography) gives the highest values of signal contrast but high testing times are necessary to detect deeper defects.
- The proposed approach for quantifying defects size (based on the signal standard deviation contrast) provides better results with respect to the literature one based on the signal contrast.
- Threshold values < 0.5 are required on the signal contrast to obtain errors within 10% in defects size evaluation.

Acknowledgments: This work is part of the Italian MIUR Project CAMPUS MANUFACTURING (Ref. DM54668).

References

[1] Baker S, Dutton S, Kelly D. Composite Materials for aircraft Structures. American Institute for Aeronautics and Astronautics, Ins., Reston, Virginia, 2004.

[2] Nikishkov Y, Airoldi L, Makeev A, Measurement of voids in composites by X-ray Computed Tomography. Composites Science and Technology, 2013; 89:89-9.

[3] Hosu MV, Murthy CRL, Ramamurthy TS, Shet A, Estimation of impact-induced damage in CFRP laminates through ultrasonic imaging. NDT&E International, 2013; 31(5):359-16.

[4] Castellano A, Fraddosio A, Piccioni MD, Ultrasonic goniometric immersion tests for the characterization of fatigue post-LVI damage induced anisotropy superimposed to the constitutive anisotropy of polymer composites. Composites Part B: Engineering, 2017; 116:, 122-15.

[5] Castellano A, Fraddosio A, Marzano S, Piccioni MD, Some advancements in the ultrasonic evaluation of initial stress states by the analysis of the acoustoelastic effect. Procedia Engineering, 2017; 199:1519-8.

[6] Tamborrino R, Palumbo D, Galietti U, Aversa P, Chiozzi S, Luprano VAM, Assessment of the effect of defects on mechanical properties of adhesive bonded joints by using non destructive methods. Composites Part B, 2016; 91:337-9.

[7] De Angelis G, Meo M, Almond, DP, Pickering SG, Angioni SL, A new technique to detect defect size and depth in composite structures using digital shearography and unconstrained optimization. NDT&E International, 2012; 45:91-6.

[8] Pérez MA, Gil L, Oller S, Impact damage identification in composite laminates using vibration testing. Composite Structures, 2014; 108:267-10.

[9] Angelidis N, Irving PE, Detection of impact damage in CFRP laminates by means of electrical potential techniques. Composites Science and Technology, 2007; 67:594-11.

[10] Maldague XPV, Theory and practice of infrared technology of non-destructive testing. John Wiley & Sons, Inc, ISBN 0-471-18190-0, 2001.

[11] Meola C, Carlomagno GM, Squillace A, Giorleo G, Non-destructive Control of Industrial Materials by means of Lock-in Thermography. Measurement Science and Technology, 2002; 10:1583-8.

[12] Usamentiaga R, Venegas P, Guerediaga J, Vega L, Lòpez I, Feature extraction and analysis for automatic characterization of impact damage in carbon fiber composites using active thermography. NDT&E International, 2013; 54:123-10.

[13] Ibarra-Castanedo C, Quantitative Subsurface Defect Evaluation by Pulsed Phase Thermography: depth Retrieval With the Phase, Ph.D. thesis, Université Laval, 2005.

[14] Ruizhen Y, Yunze H, Optically and non-optically excited thermography for composites: A review. Infrared Physics & Technology, 2016; 75:26-24.

[15] Badghaish AA, Fleming DC, Non-destructive Inspection of Composites Using Step Heating Thermography, 2008; 42:1337-21.

[16] Yunze H, Ruizhen Y, Hong Z, Deqiang Z, Gang W, Volume or inside heating thermography using electromagnetic excitation for advanced composite materials. International Journal of Thermal Sciences, 2017; 111:41-8.

[17] Garnier C, Pastor M., Eyma F, Lorrain B, The detection of aeronautical defects in situ on composite structures using Non Destructive Testing. Composite Structures 2011; 93:1328-9.

[18] Tashan R, Al-mahaidi R, Investigation of the parameters that influence the accuracy of bond defect detection in CFRP bonded specimens using IR thermography. Composite Structures, 2012; 94:519-13.

[19] Taillade F, Quiertant M, Benzarti K, Aubagnac C, Shearography and pulsed stimulated infrared thermography applied to a nondestructive evaluation of FRP strengthening systems bonded on concrete structures. Construction and Building Materials, 2011; 25:568-7.

[20] Omar M, Hassan M, Donohue K, Saito K, Alloo R, Infrared thermography for inspecting the adhesion integrity of plastic welded joints. NDT & E International, 2006; 39:1-7.

[21] Genest M, Martinez M, Mrad N, Renaud G, Fahr A, Pulsed thermography for non-destructive evaluation and damage growth monitoring of bonded repairs. Composite Structures, 2009; 88: 112-8.

[22] Krstulovic-Opara L, Klarin B, Neves P, Domazet Z, Thermal imaging and Thermoelastic Stress Analysis of impact damage of composite materials. Engineering Failure Analysis, 2011; 18:713-7.

[23] Palumbo D, De Finis R, Demelio GP, Galietti U, A new rapid thermographic method to assess the fatigue limit in GFRP composites. Composite Part B, 2016; 103:60-7.

[24] Palumbo D, De Finis R, Demelio GP, Galietti U, Study of damage evolution in composite materials based on the Thermoelastic Phase Analysis (TPA) method. Composite Part B, 2017; 117:49-12.

[25] Palumbo D, Galietti U, Damage investigation in composite materials by means of new thermal data processing procedures. Strain, 2016; 52(4):276-10.

[26] Pitarresi G, Lock-In Signal Post-Processing Techniques in Infra-Red Thermography for Materials Structural Evaluation. Experimental Mechanics 2015; 55(4):667-14.

[27] Pitarresi G, Thermal NDE of thick GRP panels by means of a Pulse modulated lock-in thermography technique. 14th International Conference on Experimental Mechanics, ICEM 2014, Poitiers, France, 4-9 July 2010. EPJ Web of Conferences, Volume 6, 9 June 2010, Article number 38014.

[28] Mulaveesala R, Tuli S, Theory of frequency modulated thermal wave imaging for non destructive subsurface defect detection. Applied Physics Letters; 2006; 89, no. 191913.

[29] Vavilov VP, Burleigh DD, Review of pulsed thermal NDT: Physical principles, theory and data processing. NDT&E International, 2015; 73:28-25.

[30] Shepard S, Advances in pulsed thermography. Proceedings of SPIE, Thermosense-XXIII, 4360, 511, 2001.

[31] Balageas, D, Roche JM, Common tools for quantitative time resolved pulse and step-heating thermography – part I: theoretical basis. QIRT Journal, 2014; 11:10-19.

[32] Grinzato E, Bison PG, Marinetti S, Vavilov V, Non-destructive evaluation of delaminations in fresco plaster using transiet infrared thermography. Research in NDE, 1994; 5:257-18.

[33] Lau SK, Almond DP, Milne JM, A quantitative analysis of pulsed video thermography. NDT & E International, 1991; 24(4):195-7.

[34] Çengel YA, Introduction to Thermodynamics and heat transfer, McGraw-Hill companies, Inc, ISBN: 978-0077235659, 2007.

[35] IRTA Manual. Diagnostic Engineering Solutions (DES srl), 2015.

[36] Montgomery DC, Runger GC, Applied Statistics and Probability for Engineers. John Wiley & Sons, Inc, 2003.

[37] Balageas DL, Roche JM, Leroy H, Comparative Assessment of Thermal NDT Data Processing Techniques for Carbon Fiber Reinforced Polymers, Materials Evaluation, 2017; 75(8):1019-13.

[38] Giorleo G, Meola C, Comparison between pulsed and modulated thermography in glass-epoxy laminates. NDT&E International, 2002; 35:287-6.